Using streamlines to visualize acoustic energy flow across boundaries[a)]

David M. F. Chapman[b)]

*Defence Research and Development Canada-Atlantic, P.O. Box 1012, Dartmouth,
Nova Scotia B2Y 3Z7, Canada*

For spherical waves that radiate from a point source in a homogeneous fluid and propagate across a plane boundary into a dissimilar homogeneous fluid, the acoustic field may differ significantly from the geometric acoustic approximation if either the source or receiver is near the interface (in acoustic wavelengths) or if the stationary phase path is near the critical angle. In such cases, the entire acoustic field must be considered, including inhomogeneous waves associated with diffraction (i.e., those components that vanish with increasing frequency). The energy flow from a continuous-wave monopole point source across the boundary is visualized by tracing acoustic streamlines: those curves whose tangent at every point is parallel to the local acoustic intensity vector, averaged over a wave cycle. It is seen that the acoustic energy flow is not always in line with the "Snell's law" or stationary phase path. Also, plots of acoustic energy streamlines do not display unusual behavior in the vicinity of the critical angle. Finally, it is shown that there exists a law of refraction of acoustic energy streamlines at boundaries with density discontinuities analogous to Snell's law of refraction of ray paths across sound speed discontinuities. Examples include water-to-seabed transmission and water-to-air transmission.
© 2008 Acoustical Society of America. [DOI: 10.1121/1.2931956]

I. INTRODUCTION

Geometric ray tracing, which is based on an approximation to solutions of the acoustic wave equation, provides an intuitive visualization of propagation of an acoustic field from source to receiver,[1] but has limitations. Being the high-frequency limit of the solution, geometric ray theory does not include diffracted components of the field. Also, geometric rays only coincide with the direction of energy flow when the medium has slowly varying properties and negligible reflection and diffraction. To correctly determine energy flow, the full wave-theory solution to the acoustic wave equation (with appropriate boundary conditions) is required, including reflected and diffracted components of the field. However, it would be instructive to have a raylike visualization of the acoustic field that portrays the propagation of energy from source to receiver, especially in cases where diffraction and/or reflection significantly alter the field. Such a visualization is provided by the acoustic energy streamline (also called the acoustic streamline or the intensity streamline). The acoustic energy streamline is the curve which at every point is tangent to the direction of the local average acoustic intensity vector, that is, the product of acoustic pressure and acoustic particle velocity averaged over one wave cycle.[2]

The acoustic streamline is not a new concept, having previously been applied to homogeneous media with multiple coherent sources and nearby boundaries. Waterhouse *et*

al.[3,4] introduced continuous streamlines as an alternative to grids of intensity vectors. Skelton and Waterhouse[5] and Zhang and Zhang[6] applied the method of Ref. 3 to radiation from a spherical shell. These papers established not only that sound energy from cw sources propagates along streamlines but also that adjacent streamlines constitute a streamline tube of energy flow, as there is no energy flow across streamlines. In this way, the magnitude of acoustic intensity varies inversely as the cross-sectional area of the streamline tube, a property already employed in ray acoustics.[7]

In this paper, the acoustic streamline concept is applied to problems involving propagation of acoustic waves across fluid-fluid boundaries, that is, propagation from a continuous-wave (cw) monopole source in a semi-infinite homogeneous fluid medium having a plane boundary with a second semi-infinite homogenous fluid medium with different density and sound speed. Specifically, two examples are considered: water-to-seabed transmission and water-to-air transmission. The acoustic fields and streamlines in these relatively simple environments provide a variety of sometimes surprising physical results.

At the outset it should be emphasized that, unlike rays, streamlines do not represent alternate solutions or approximations to the acoustic field. The acoustic field must be known for streamlines to be traced. Thus, there are no savings in computational time or efficiency; there is only the benefit of an improved visualization of the average energy flow in the acoustic field.

The current analysis is restricted to cw fields. In the case of time-dependent fields (pulse propagation, for example) involving multipaths with different times of flight, geometric

---

Report Documentation Page

Public reporting burden for the collection of information is estimated to average 1 hour per response, including the time for reviewing instructions, searching existing data sources, gathering and maintaining the data needed, and completing and reviewing the collection of information. Send comments regarding this burden estimate or any other aspect of this collection of information, including suggestions for reducing this burden, to Washington Headquarters Services, Directorate for Information Operations and Reports, 1215 Jefferson Davis Highway, Suite 1204, Arlington VA 22202-4302. Respondents should be aware that notwithstanding any other provision of law, no person shall be subject to a penalty for failing to comply with a collection of information if it does not display a currently valid OMB control number.

1. REPORT DATE **15 APR 2008**	2. REPORT TYPE	3. DATES COVERED **00-00-2008 to 00-00-2008**

4. TITLE AND SUBTITLE **Using streamlines to visualize acoustic energy flow across boundaries**	5a. CONTRACT NUMBER
	5b. GRANT NUMBER
	5c. PROGRAM ELEMENT NUMBER
6. AUTHOR(S)	5d. PROJECT NUMBER
	5e. TASK NUMBER
	5f. WORK UNIT NUMBER
7. PERFORMING ORGANIZATION NAME(S) AND ADDRESS(ES) **Defence Research and Development Canada -Atlantic,PO Box 1012,Dartmouth, Nova Scotia B2Y 3Z7, Canada,**	8. PERFORMING ORGANIZATION REPORT NUMBER
9. SPONSORING/MONITORING AGENCY NAME(S) AND ADDRESS(ES)	10. SPONSOR/MONITOR'S ACRONYM(S)
	11. SPONSOR/MONITOR'S REPORT NUMBER(S)

12. DISTRIBUTION/AVAILABILITY STATEMENT **Approved for public release; distribution unlimited**

13. SUPPLEMENTARY NOTES

14. ABSTRACT

15. SUBJECT TERMS

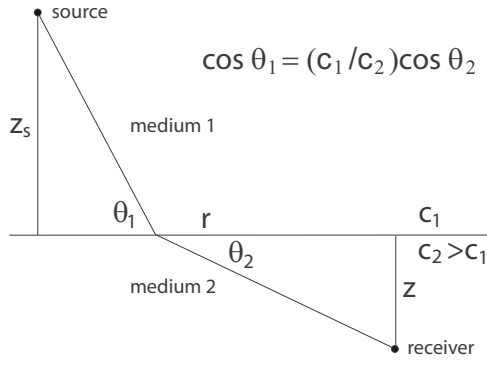| 16. SECURITY CLASSIFICATION OF:			17. LIMITATION OF ABSTRACT **Same as Report (SAR)**	18. NUMBER OF PAGES **9**	19a. NAME OF RESPONSIBLE PERSON
a. REPORT **unclassified**	b. ABSTRACT **unclassified**	c. THIS PAGE **unclassified**			

FIG. 1. Geometry of transmission from a point source in one homogeneous medium to a receiver in another, separated by a plane boundary, the case $c_2 > c_1$.

ray paths and acoustic streamlines are more likely to coincide as the pulse components propagating via the multipaths may not overlap at the receiver; however, diffraction may still have a role to play in time-dependent fields. Even for cw fields, streamlines and rays can be practically the same particularly in slowly varying media away from reflectors and diffractors.

The analysis below is limited to fluid media. Although it would be more realistic (and likely interesting) to include the elastic properties of the lower medium in the water-to-seabed case, these properties are assumed to be not important for the purpose at hand. This is a common approximation made when the seabed is unconsolidated sediment.[8]

II. THEORY

A. Integral representation of acoustic fields

Referring to Fig. 1, consider a homogeneous fluid halfspace of density ρ_1 and sound speed c_1 in contact with a second (lower) homogeneous fluid half-space of density, $\rho_2 = g\rho_1$, and sound speed, $c_2 = c_1/n$, separated by the plane boundary, $z = 0$. (That is, the lower:upper density ratio is g and the upper:lower speed ratio, or index of refraction, is n.) A monopole cw source of angular frequency ω is placed in the upper medium at height $z = z_s$, and the receiver could either be in the upper medium ($z > 0$) or the lower medium ($z < 0$) at horizontal range r. The exact wave-theory solution for the acoustic potential is well-known;[9] however, there is no straightforward functional form, only a representation based on expanding the spherical waves into an integral over plane waves traveling in all directions. Taking advantage of the cylindrical symmetry, the incident acoustic velocity potential reduces to the single integral

$$\Psi_{inc} = \frac{e^{ik_1\sqrt{r^2+|z_s-z|^2}}}{\sqrt{r^2+|z_s-z|^2}}$$
$$= \frac{ik_1}{2\pi}\int_{i\infty}^{\pi/2} J_0(k_1 r \cos\theta)e^{ik_1|z_s-z|\sin\theta}\cos\theta d\theta$$
$$(z > 0), \tag{1}$$

in which J_0 is the Bessel function of zero order, $k_1 = \omega/c_1$ is the wavenumber in medium 1, and θ is the integration variable. (There is an implied time factor $e^{-i\omega t}$.) Note that the

incident potential has a source singularity at $(r, z) = (0, z_s)$, a fact which has computational consequences.

The integration contour runs from $+i\infty$ in the θ-plane along the positive imaginary axis to the origin and then along the real axis to $\pi/2$. Equation (1) represents an integral over cylindrical waves with horizontal wavenumber $k_1 \cos\theta$ and vertical wavenumber $k_1 \sin\theta$, so θ represents the grazing angle of the wave relative to the boundary plane. Waves associated with real θ are the familiar homogeneous waves (constant amplitude along constant phase fronts), while waves associated with imaginary θ are inhomogeneous waves[10] (evanescent amplitude along constant phase fronts).[11] Inhomogeneous waves are necessary to represent the near field of the point source and diffracted components of the reflected and transmitted fields. There exists an alternate—yet mathematically equivalent—formulation that uses wavenumber integration, a basis for several computational wave propagation codes.[12–14]

The reflected potential (which must be added to the incident potential to represent the entire field in the upper medium) is

$$\Psi_{refl} = \frac{ik_1}{2\pi}\int_{i\infty}^{\pi/2} J_0(k_1 r \cos\theta)e^{ik_1(z_s+z)\sin\theta}R(\theta)\cos\theta d\theta$$
$$(z > 0) \tag{2a}$$

and the transmitted potential (the entire field in the lower medium) is

$$\Psi_{trans} = \frac{ik_1}{2\pi g}\int_{i\infty}^{\pi/2} J_0(k_1 r \cos\theta)e^{ik_1(z_s\sin\theta - z\sqrt{n^2-\cos^2\theta})}$$
$$\times T(\theta)\cos\theta d\theta \quad (z < 0), \tag{2b}$$

in which z is positive upward and $R(\theta)$ and $T(\theta)$ are the familiar plane-wave reflection and transmission coefficients for pressure, respectively,

$$R(\theta) = \frac{g\sin\theta - \sqrt{n^2-\cos^2\theta}}{g\sin\theta + \sqrt{n^2-\cos^2\theta}} \tag{3a}$$

and

$$T(\theta) = \frac{2g\sin\theta}{g\sin\theta + \sqrt{n^2-\cos^2\theta}}. \tag{3b}$$

The acoustic pressure and two components of particle velocity in either medium are given by

$$p = \rho\frac{\partial\Psi}{\partial t} = -i\omega\rho\Psi, \tag{4a}$$

$$v_r = -\frac{\partial\Psi}{\partial r}, \tag{4b}$$

$$v_z = -\frac{\partial\Psi}{\partial z}. \tag{4c}$$

In this paper, the integrals in Eqs. (2a) and (2b) will be evaluated numerically, so the derivatives in Eqs. (4a)–(4c) need to be applied before the integration. Note the factor g in the denominator of Eq. (2b); this is needed to ensure that

both the pressure and the vertical component of the particle velocity are continuous at the boundary, and it also governs the ratio of the horizontal components of particle velocity on either side of the boundary, as will be seen in Sec. V.

B. Asymptotic evaluation, phase functions, and Snell's law

Brekhovskikh[9] and Brekhovskikh and Godin[12] derive the geometric acoustics limit of the reflected and transmitted fields, using Eqs. (2a) and (2b) as starting points, applying the method of steepest descent. These results are not necessary for the streamline calculations below, but the stationary phase paths are of interest, as they are the geometric ray paths. Because the media are homogeneous, the ray paths in both media are straight line segments with associated grazing angles.

For a receiver in the upper medium, the rays are simply straight lines: (a) for the direct path, a straight line from the source at height z_s above the boundary to the receiver at horizontal distance r and height z, and (b) for the reflected path, a straight line from the image source at depth z_s below the boundary to the same receiver in the upper medium straightforward. This image construction ensures that the angle of incidence equals the angle of reflection for the reflected ray, a straightforward consequence of the stationary phase condition applied to the reflected field.

For a receiver in the lower medium, the phase of the transmitted field is

$$\Phi_{trans} = k_1 r \cos\theta + k_1(z_s \sin\theta - z\sqrt{n^2 - \cos^2\theta}) \quad (z < 0). \tag{5}$$

The geometric ray angles follow from the stationary phase condition, that is, $\partial\Phi/\partial\theta = 0$. In this case, the stationary phase path is given by

$$r = z_s \cot\theta_1 - z\cos\theta_1/\sqrt{n^2 - \cos^2\theta_1}$$
$$= z_s \cot\theta_1 - z\cot\theta_2, \tag{6}$$

in which θ_1 is the ray angle in the upper medium and θ_2 is the ray angle in the lower medium, given by

$$\cos\theta_1 = n\cos\theta_2, \tag{7}$$

which is Snell's law of refraction.[15] For a given source-receiver geometry, Eq. (6) is numerically solved for θ_1 and then Eq. (7) gives θ_2. In the geometric acoustic approximation, the wavefront is perpendicular to the ray, and the particle velocity is parallel to the ray. Later, these geometric ray propagation angles will be compared to the direction of energy flow.

C. Critical angle

Note that for $n < 1$ there is a critical angle $\theta_c = \cos^{-1} n$ dividing the range of θ into two regions: $\theta > \theta_c$ and $\theta < \theta_c$. In the absence of absorption, for $\theta > \theta_c$, the vertical wavenumber in the lower medium is real, and the reflection and transmission coefficients are real. In this domain of angles, the reflected and transmitted plane waves are homogeneous, and the reflected wave has reduced amplitude. For $\theta < \theta_c$, the

vertical wavenumber in the lower medium is imaginary, and the reflection and transmission coefficients are complex. The reflected plane wave is homogeneous (with a phase shift and unreduced amplitude) and the transmitted plane wave is inhomogeneous. The presence of these inhomogeneous transmitted waves just beneath the boundary has significant influence on the energy flow there and have, in fact, been observed in nature[16] and in propagation models.[17–19]

Conventionally, absorption in either medium is introduced by adding a small negative imaginary component to the corresponding sound speed. [If $c \rightarrow c(1 - i\varepsilon)$, the attenuation in dB/wavelength becomes $(40\pi \log_{10} e)\varepsilon \approx 54.6\varepsilon$.] The index of refraction, reflection coefficient, and transmission coefficient become generally complex. Waves that are purely homogeneous or purely inhomogeneous retain their principle characteristics but acquire a small dose of the opposite characteristics.

III. METHOD OF COMPUTATION

All computations are performed in MATHEMATICA 6 (Ref. 20) on a typical laptop computer with an Intel Pentium 2 GHz processor.

A. Calculating acoustic field variables

The computation of the acoustic field necessarily depends on whether the field point is on the same side of the boundary as the source or the other side of the boundary. Assuming the source is in the upper medium, if the receiver is also in the upper medium, the total field is the sum of the incident field and the reflected field; if the receiver is in the lower medium, the total field is simply the transmitted field.

When needed, the field values for pressure and particle velocity are computed from Eqs. (1), (2a), and (2b). In the upper medium, $\Psi_1 = \Psi_{inc} + \Psi_{ref}$. The incident field Ψ_{inc} has analytic form, so no integration is needed, as Eqs. (4a)–(4c) can be applied directly and the result can be evaluated. (In principle, the integral for the incident field could be combined with the integral for the reflected field, but this introduces instabilities in the numerical integral in the vicinity of the source singularity.) For the reflected field Ψ_{refl}, the integral in Eq. (2a) is numerically calculated, applying Eqs. (4a)–(4c) to the integrand first. In the lower medium, $\Psi_2 = \Psi_{trans}$, and again Eqs. (4a)–(4c) must be applied to the integrand of Eq. (2b) first. The calculation uses the MATHEMATICA function NIntegrate, an adaptive algorithm that subdivides the range and chooses the appropriate method according to the nature of the integral. Integration over real-valued angles and imaginary-valued angles must be performed separately, and the latter integral must be truncated at a finite value (of the order 100 divided by the source frequency in kilohertz, enough to span significant contributions from inhomogeneous waves). Although the integrands are naturally oscillatory, this poses no difficulty for MATHEMATICA at the low frequencies where diffraction effects are significant. (Poor convergence is flagged by MATHEMATICA, which also suggests remedies.) Including realistic values of acoustical absorption dampens the oscillations somewhat and aids convergence. For a given environ-

ment, all three acoustic field variables at a point are calculated in about a second.

B. Acoustic intensity of a continuous-wave field

The instantaneous acoustic intensity (the vector of acoustic energy flux) is the product of pressure and velocity.[21] For a cw field, writing the acoustic potential in terms of real-valued amplitude and phase functions,

$$\Psi(\mathbf{x},t) = A(\mathbf{x})e^{i[\Phi(\mathbf{x})-\omega t]}, \tag{8}$$

the instantaneous intensity is, from Eqs. (4a)–(4c)

$$\mathbf{j} = \operatorname{Re} p \operatorname{Re} \mathbf{v} = \rho\omega A^2 \nabla \Phi \sin^2[\Phi - \omega t]$$
$$- \rho\omega A \nabla A \sin[\Phi - \omega t]\cos[\Phi - \omega t]. \tag{9}$$

Note that the instantaneous intensity is the sum of a pulsating (nonreversing) component in the direction of the gradient of phase and an oscillatory (zero-average) component in the direction of the gradient of amplitude. Averaging over one cycle of time, the average intensity is[22]

$$\langle \mathbf{j} \rangle = \tfrac{1}{2}\rho\omega A^2 \nabla \Phi \equiv \tfrac{1}{2}\operatorname{Re} p^*\mathbf{v}. \tag{10}$$

The average intensity governs the net transport of energy, which is in the direction of the gradient of phase. The instantaneous intensity is always in the direction of the particle velocity, which may not be the same as the direction of net energy flow. This is discussed by D'Spain *et al.* in detail.[23] For visualizing net energy flow, it is the average intensity that is relevant.[24]

C. Tracing acoustic streamlines

Acoustic streamlines are tangent everywhere to the direction of the local average intensity vector, so the first step in tracing streamlines is to calculate the acoustic intensity and determine its orientation. For monopole sources in layered media, we can restrict our view to the single plane containing source and receiver. The grazing angle of the average intensity vector is (after Ref. 3)

$$\varphi = \tan^{-1}(\langle j_z \rangle/\langle j_r \rangle), \tag{11}$$

and the differential equation of the streamline in parametric form is

$$dz/ds = \sin \varphi(r,z), \tag{12a}$$

$$dr/ds = \cos \varphi(r,z), \tag{12b}$$

in which ds is the element of arc length along the streamline. The streamline is traced in a simple two-stage marching-style solution based on algorithm with stepsize Δs

$$\hat{z}_i = z_i + \tfrac{1}{2}\Delta s \sin \varphi(r_i,z_i), \tag{13a}$$

$$\hat{r}_i = r_i + \tfrac{1}{2}\Delta s \cos \varphi(r_i,z_i), \tag{13b}$$

$$z_{i+1} = z_i + \Delta s \sin \varphi(\hat{r}_i,\hat{z}_i), \tag{13c}$$

$$r_{i+1} = r_i + \Delta s \cos \varphi(\hat{r}_i,\hat{z}_i). \tag{13d}$$

In words: From a given point (r_i,z_i), the direction $\varphi(r_i,z_i)$ of the intensity vector is determined, and a half step $\Delta s/2$ is taken in that direction to a provisional point $(\hat{r}_i,\hat{z}_i)$. At this provisional point, a revised direction $\varphi(\hat{r}_i,\hat{z}_i)$ of the intensity vector is determined. Finally, a full step Δs is taken from the original point (r_i,z_i) in the direction $\varphi(\hat{r}_i,\hat{z}_i)$. The final position (r_{i+1},z_{i+1}) is the estimated next point on the streamline. Without the half step, this would be the Euler method; the modification using the half step has lower error. Overall error is minimized by making the step size sufficiently small.

In practice, a variable step size Δs is used that adapts to the local curvature of the streamline. The distance between the provisional point $(\hat{r}_i,\hat{z}_i)$ and the point halfway between the original point (r_i,z_i) and the final point (r_{i+1},z_{i+1}) is compared to two threshold values, t_1 and t_2, with $t_1 < t_2$. As long as

$$t_1 < |(r_{i+1}-r_i,z_{i+1}-z_i)/2 - (\hat{r}_i-r_i,\hat{z}_i-z_i)| < t_2, \tag{14}$$

the step size is maintained; should the difference drop below t_1, the step size is increased to speed up the streamline tracing; should the difference exceed t_2 the step size is reduced to improve accuracy. In this paper, in which the source-receiver distance is only a few meters, the starting step size is typically 0.05 m, the error thresholds are of the order 10^{-4} m, and $t_2 = 2t_1$. When needed, the step size is altered up or down by the factor of $\sqrt{2}$. The number of steps required to trace a streamline can vary between around 10 to several hundred, depending on the geometry, source frequency, and complexity of the field.

When the streamline crosses a density discontinuity, care must be taken to account for the discontinuous change of direction that occurs. (The law of streamline refraction at boundaries will be discussed in Sec. V.) If the new point lies across the boundary from the previous point, the crossing position is interpolated and that becomes the new point. The step size is reduced and the calculation resumes in the new medium.

In the case of multipath interference, the structure of the acoustic field becomes finer as frequency increases and wavelength decreases. The steps of a streamline trace become smaller and smaller. This makes streamline tracing in such cases more expensive, computationally speaking, as frequency increases. On the other hand, when there are no multipaths, the amplitude of any diffracted field component decreases with increasing frequency, so convergence to the high-frequency limit is more rapid in this case.

The above streamline tracing method is elementary, and without a doubt it could be improved upon for speed while maintaining accuracy; however, it is adequate for the purpose at hand, and is validated by tracing streamlines in both directions, discussed below.

1. Streamline between source and receiver

To trace a streamline between source and a receiver at a specified location, the initial field point is chosen to be the receiver location, the direction of travel is deemed to be the opposite of the intensity vector, and the streamline tracing

procedure outlined above (presumably) finds its way back to the source. As the source is approached, the incident spherical-wave field dominates, becoming a "sink" for the streamline. The calculation is terminated at a point suitably close to the source. To check the calculation, the streamline is relaunched at the terminal point, with the direction of travel the same as the intensity vector. If the initial step size and error tolerances are chosen well, the return streamline will pass the receiver at an acceptably small distance. Some tuning of the numerical parameters is needed to achieve convergence, which is judged by eye. This procedure is a necessary check if streamline fans are to be computed.

2. Tracing of streamline fans

A streamline fan is a group of streamlines launched from the source, usually at equally spaced angles around a central streamline. According to the development in this paper, sound energy from cw sources propagates along streamlines; therefore streamlines in a streamline fan can be viewed as cross sections of streamline tubes of equal energy flow, as there is no energy flow across the tube wall. In this way, the downstream spacing of streamlines provides an indication of the relative intensity (see Ref. 4). To ensure this interpretation, the launch radius must be sufficiently small that any reflected field is insignificant at the launch point; for the computations in this paper, a launch radius of about 1/20 of the source-boundary distance is used and the ratio of reflected to incident field is verified to be less than 1/100 before proceeding. Highly dissimilar media demand a smaller launch radius, owing to the strong reflection from the boundary.

IV. COMPUTED EXAMPLES

Two examples of cross-boundary acoustic transmission are provided: one water-to-sediment and the other water-to-air. In each case, 31 streamlines or rays are launched into 180°, 6° apart.

A. Water-to-sediment transmission

For the water-to-sediment example, inspired by the SAX04 experiment,[25,26] the environment used is $c_1 = 1531$ m/s, $c_2 = 1687$ m/s, sediment attenuation $= 0.23$ dB/wavelength, and $g = 2.02$. (That is, $c_2 = 1687 - 7.1i$ m/s or $n = 0.9075 + 0.0038i$.) The critical angle ($\text{Re}[\cos^{-1} n]$) for this environment is $\theta_c = 24.8°$. The source is at height $z_s = 2.58$ m. (In the experiment, the sensors were between 7 and 9 m from the source at less than 1 m depth.) Figures 2(a)–2(c) show the streamline fans at frequencies of 150, 500, and 1500 Hz. Figure 2(d) shows the corresponding ray fan.

Whereas the geometric ray paths are straight lines, the streamlines are, in general, curved, owing to constructive interference between waves. Note that the streamlines may cross the critical ray (heavy dashed line), that is, the ray incident at the critical angle. Also note the discontinuous change in streamline direction at the boundary. (This is discussed in Sec. V in detail.)
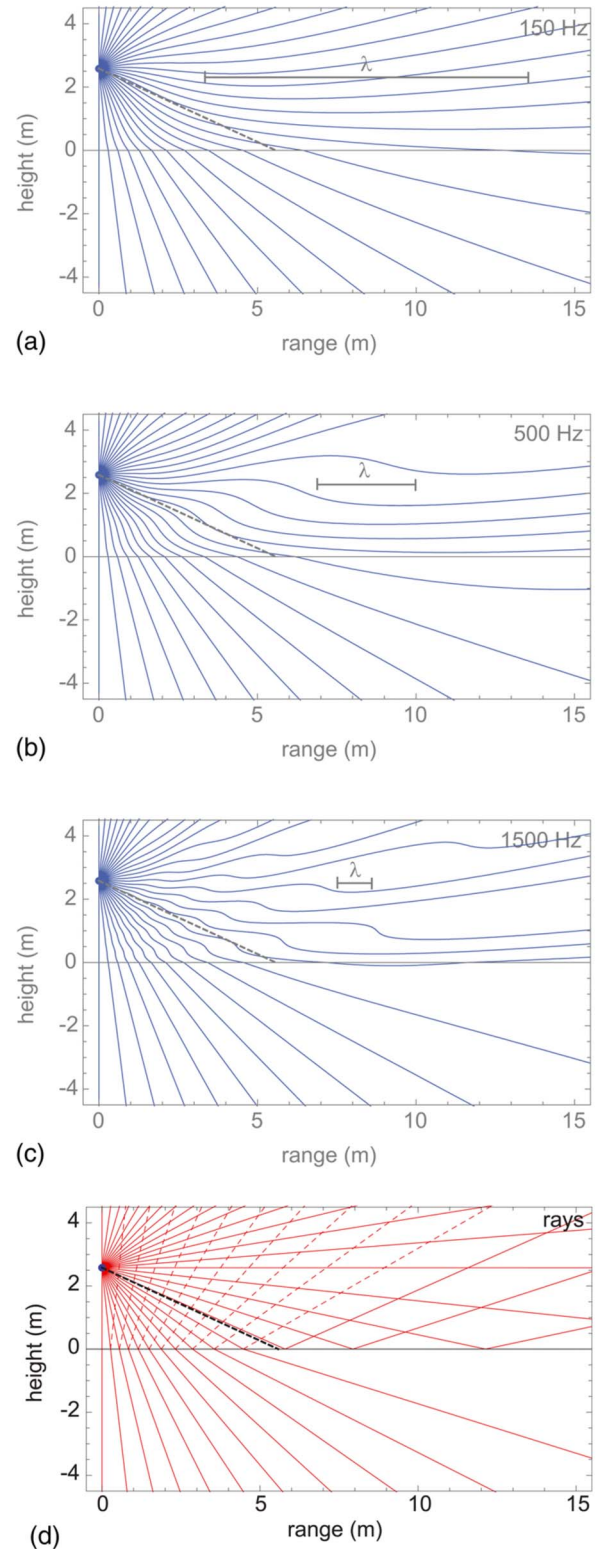

FIG. 2. (Color online) Streamlines of energy flow for water-to-sediment transmission: (a) 150 Hz, (b) 500 Hz, (c) 1500 Hz, and (d) the corresponding ray paths. Solid lines: streamlines [(a)–(c)] or incident, transmitted, and totally reflected rays (d). Dashed lines: partially reflected rays. Heavy dashed line: critical ray. Associated acoustic wavelengths in water: (a) 10.2 m, (b) 3.1 m, (c) 1.0 m.

The structure of the field in the upper medium becomes increasingly complicated as frequency increases, owing to the interference of the incident and reflected fields at shorter

wavelengths. As frequency increases in a cw multipath environment, a streamline will not converge to a ray, unless all other paths are increasingly attenuated; however, the streamline should converge to a limiting trajectory around which the streamline weaves with fine scale structure. There is evidence of this in Fig. 2(c), particularly for those streamlines that enter the sediment.

In regions where streamlines have significant curvature, linear extrapolation of the local intensity vector would not be a good indicator of the path of energy transport to that point. One even sees streamlines enter the lower medium and then turn back and return to the upper medium well downstream. This return of energy to the upper medium is reminiscent of "head waves" or "lateral waves" that travel substantially at the speed of the lower medium but are sensed in the upper medium, and which have practical application in seismoacoustic inversion.[26]

Beyond the point at which the critical ray ends, just under the boundary, ray theory predicts a "shadow zone" of low intensity. Diffractive wave corrections to ray theory[27] in this region can be interpreted as a vertically inhomogeneous wave traveling horizontally in the lower medium, associated with a perfectly reflected ray striking the boundary. This inhomogeneous wave is strongest at the boundary, penetrates deeply at lower frequencies and vanishes in the limit of infinite frequency. The streamline visualization of this phenomenon in Figs. 2(a)–2(c) shows that the energy in this region actually enters the lower medium considerably upstream of the measurement point, resolving the apparent contradiction that a ray could be perfectly reflected yet still transmit a sensible signal.

In the lower medium, there are only transmitted waves, both refracted and diffracted, without the complication of reflected waves. At all frequencies shown, in the region beneath the source, the streamlines are nearly straight, owing to the dominance of the geometrically refracted field there. Further downstream, the stronger influence of the inhomogeneous waves of the diffracted component causes the streamlines to curve more upward as the boundary is approached. The transition between the refracted-dominated field and the diffraction-dominated field is gradual at the lowest frequency shown [Fig. 2(c)]. At the highest frequency shown [Fig. 2(c)], there is a more obvious demarcation between these extremes, as one would expect as the geometric acoustic limit is approached [compare to Fig. 2(d)].

Detailed directional differences between geometric rays and intensity vectors are difficult to see by simply comparing streamline fans with ray fans. To more clearly demonstrate the difference between the direction of the geometric ray through a point and the direction of the acoustic intensity at that point, their differences (ray minus intensity) at three frequencies are plotted in Figs. 3(a)–3(c) as two-dimensional contour plots spanning the lower medium. Positive values indicate where the ray direction is steeper than the associated streamline and vice versa. Note that there is an island of negative values (streamlines steeper than rays) just beneath the point where the critical ray joins the boundary; this island shrinks with increasing frequency. Further downstream, there is generally a region of positive values (rays steeper than
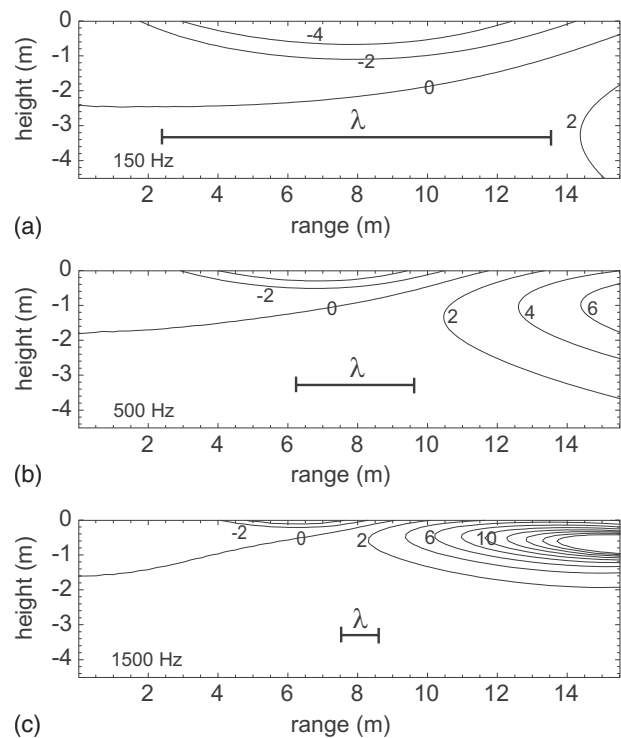

FIG. 3. Contour plots of ray direction minus intensity vector direction (in degrees) in the lower medium for water-to-sediment transmission. (a) 150 Hz, (b) 500 Hz, and (c) 1500 Hz. Positive values: rays steeper than streamlines. Negative values: streamlines steeper than rays. Associated acoustic wavelengths in sediment: (a) 11.2 m, (b) 3.4 m, and (c) 1.1 m.

streamlines). The directional differences in this region grow remarkably large in this region as frequency increases, yet it should be recalled from Figs. 2(a)–2(c) that the magnitude of the intensity is quite small there. This feature disappears as frequency is increased to 5000 Hz (not illustrated). Overall, for the transmitted wave, one can see that the direction of the intensity tends to coincide more with the direction of the geometric ray path as frequency increases. Even so, directional measurements with intensity probes should be interpreted with caution with respect to the path along which the signal arrived.

B. Water-to-air transmission

For the water-to-air example, inspired by recent interest in anomalous acoustic transparency of the water/air boundary,[28] the environment used is $c_1=1500$ m/s, $c_2=330$ m/s, and $g=0.001\,25$. (That is, $c_2=330-0.06i$ m/s or $n=4.5454+0.0008i$.) A very mild absorption coefficient of 0.01 dB/wavelength is included to stabilize the calculation. The source is at height $z_s=0.5$ m in water. (The air layer is placed below to aid comparison with the previous water-to-sediment case.) Figures 4(a)–4(c) show the streamline fans at frequencies of 15, 150, and 1500 Hz. Figure 4(d) shows the corresponding ray fan.

This sequence of streamline fans shows the strong frequency sensitivity of anomalous transmission of sound from water to air. Godin et al.[26] explains how incident inhomogeneous waves in the near field of the source interfere with inhomogeneous waves reflected by the boundary with the result that significant energy can be transmitted across the
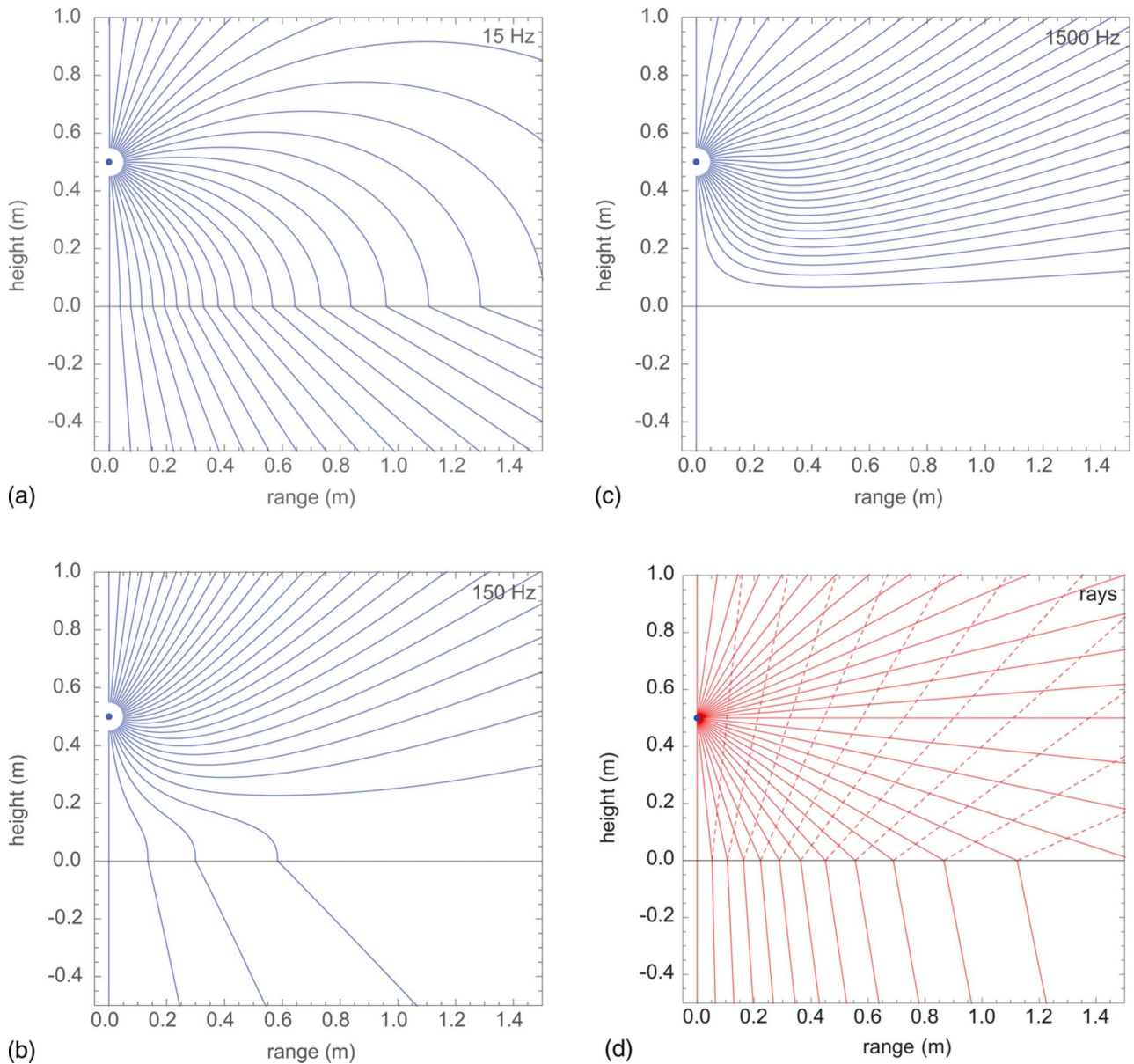
FIG. 4. (Color online) Streamlines of energy flow for water-to-air transmission (note that the water is *above* the air): (a) 15 Hz, (b) 150 Hz, and (c) 1500 Hz. Solid lines in (a)–(c): streamlines. Solid lines in (d): incident and transmitted rays. Dashed lines in (d): partially reflected rays. Associated acoustic wavelengths in water: (a) 100 m, (b) 10 m, and (c) 1 m.

boundary at very low frequencies. This is considered anomalous because this high impedance contrast (mostly due to the 800-fold density ratio) conventionally implies that the boundary would act as an acoustic mirror. As frequency increases, more and more streamlines are turned back from the boundary until at the highest frequency shown the conventional mirrorlike nature of the boundary is restored.

In this example, the ray fan bears little resemblance to any of the three streamline fans, and hence provides little insight to the energy flow from the source. Considering the streamline trajectories, note the very large direction change at the boundary associated with the large density contrast, which will shortly be explained analytically. Also note that the transmitted streamlines, when traced back linearly, appear to emanate from the true source position, a peculiarity that is not fully understood at this time.

V. REFRACTION OF STREAMLINES AT A BOUNDARY WITH A DENSITY DISCONTINUITY

From the computed examples, it is evident that acoustic streamlines are generally curved (even in homogeneous media) according to the structure of the acoustic fields that governs them. Additionally, there appears to be discontinuous refraction of streamlines at the boundary between dissimilar fluids. In fact, this discontinuous refraction only occurs when the density changes abruptly across the boundary and this fact can be stated in the form of a refraction law analogous to Snell's law.

Since both the acoustic pressure and vertical component of particle velocity are continuous across a horizontal boundary between two fluids, it follows from Eq. (10) that the vertical component of average intensity is also continuous at the boundary:
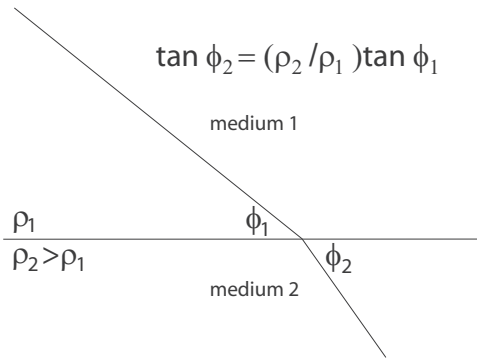
$$\tan \phi_2 = (\rho_2 / \rho_1) \tan \phi_1$$

medium 1

$\dfrac{\rho_1}{\rho_2 > \rho_1}$ ϕ_1 ϕ_2

medium 2

FIG. 5. Acoustic streamline refraction by a density discontinuity, for the case $\rho_2 > \rho_1$.

$$\langle j_{z1} \rangle = \langle j_{z2} \rangle. \tag{15}$$

The horizontal intensity components are related as well: From the integrands in Eqs. (1), (2a), and (2b), consider the acoustic field at an individual incident angle θ. From Eqs. (3a), (3b), and (4a)–(4c), the ratio of the horizontal components of particle velocity at the boundary is

$$\frac{v_{r1}(\theta)}{v_{r2}(\theta)} = \frac{1 + R(\theta)}{g^{-1} T(\theta)} = g, \tag{16}$$

Since this ratio turns out to be independent of angle, it applies equally well to the entire field (i.e., the entire integral). That is (at the boundary),

$$v_{r1} = g v_{r2}. \tag{17}$$

Again, pressure is continuous at the boundary, so the horizontal components of average intensity have the same ratio as those of the particle velocity:

$$\langle j_{r1} \rangle = g \langle j_{r2} \rangle. \tag{18}$$

Since the vertical component of average intensity is always continuous and the horizontal component of average intensity changes according to the density contrast, it follows that the streamlines must change direction at a density discontinuity. In fact, from Eq. (8),

$$\frac{\tan \varphi_2}{\tan \varphi_1} = \frac{\langle j_{z2} \rangle / \langle j_{r2} \rangle}{\langle j_{z1} \rangle / \langle j_{r1} \rangle} = g, \tag{19}$$

that is,

$$\tan \varphi_2 = g \tan \varphi_1, \tag{20}$$

as illustrated in Fig. 5. This law of streamline refraction at a boundary is comparable to Snell's law of ray refraction in Eq. (7), with the interesting difference that the streamline bends toward the denser medium, whereas the ray bends away from the faster medium. Although derived for the restricted cases considered in this paper, it is believed that the law of streamline refraction at a boundary is more generally true. (The identical argument also applies to instantaneous intensity, which is not considered in this paper.)

VI. CONCLUSIONS

An acoustic streamline is a curve whose tangent everywhere along its path is parallel to the the average local in-tensity vector. The acoustic streamline thus represents the path of mean energy flow. This concept was applied to visualize energy flow from a monopole cw source across boundaries between dissimilar fluids. Streamline fans were calculated and shown for two examples: (1) water-to-sediment transmission, typical of sediment acoustic experimentation, and (2) anomalous water-to-air transmission at infrasonic frequencies. It was observed that significant levels of diffracted waves (inhomogeneous waves) alter the energy flow significantly from what would be expected from geometrically traced rays. It was also observed that the critical angle (when one can be defined) is less relevant to energy flow as frequency decreases. A material density contrast across a boundary leads to the discontinuous bending of acoustic streamlines, governed by a law of streamline refraction at a boundary analogous to Snell's law for ray refraction, but involving the cross-boundary ratio of densities rather than the ratio of sound speeds. Potential for further work includes (1) investigating streamlines based on instantaneous intensity, leading to realistic tracing of energy propagation in pulses when interference and diffraction are significant, (2) consideration of the role of elastic properties of seabed media, and (3) consideration of the role of acoustic absorption on streamline trajectories and energy loss along their arcs.

[1] A. D. Pierce, *Acoustics: An Introduction to Its Physical Principles and Applications* (Acoustical Society of America, Melville, New York, 1989), Chap. 8, pp. 371–419.

[2] The term "streamline" is borrowed from the field of hydrodynamics, in which the streamline is the curve everywhere tangent to the direction of the local fluid velocity.

[3] R. V. Waterhouse, T. W. Yates, D. Feit, and Y. N. Liu, "Energy streamlines of a sound source," J. Acoust. Soc. Am. **78**, 758–762 (1985).

[4] R. V. Waterhouse and D. Feit, "Equal-energy streamlines," J. Acoust. Soc. Am. **80**, 681–684 (1986).

[5] E. A. Skelton and R. V. Waterhouse, "Energy streamlines for a spherical shell scattering plane waves," J. Acoust. Soc. Am. **80**, 1473–1478 (1986).

[6] J. Zhang and G. Zhang, "Analysis of acoustic radiation and scattering from a submerged spherical shell by energy streamlines," J. Acoust. Soc. Am. **88**, 1981–1985 (1990).

[7] A. D. Pierce, *Acoustics: An Introduction to Its Physical Principles and Applications* (Acoustical Society of America, Melville, New York, 1989), Chap. 8–5: pp. 396–400.

[8] K. L. Williams, D. R. Jackson, E. I. Thorsos, D. Tang, and S. G. Schock, "Comparison of sound speed and attenuation measured in a sandy sediment to predictions based on the Biot theory of porous media," IEEE J. Ocean. Eng. **27**, 413–427 (2002).

[9] L. M. Brekhovskikh, *Waves in Layered Media, Second Edition* (Academic, Orlando, 1980), Chap. IV (translated by R. T. Beyer).

[10] L. M. Brekhovskikh and O. A. Godin, *Acoustics of Layered Media I: Plane and Quasi-Plane Waves* (Springer-Verlag, Berlin, 1990), Chap. 2, p. 17.

[11] That is, $\cos(i|\theta|) = \cosh(|\theta|)$, while $\sin(i|\theta|) = i \sinh(|\theta|)$, so the oscillatory exponential in the integrand becomes an evanescent exponential.

[12] L. M. Brekhovskikh and O. A. Godin, *Acoustics of Layered Media II: Point Sources and Bounded Beams*, 2nd ed. (Springer-Verlag, Berlin, 1999), Chap. 1, pp. 1–16.

[13] F. B. Jensen, W. A. Kuperman, M. B. Porter, and H. Schmidt, *Computational Ocean Acoustics* (American Institute of Physics, New York, 1994), Chap. 4.

[14] C. H. Chapman, "A new method for computing synthetic seismograms," Geophys. J. R. Astron. Soc. **54**, 481–518 (1978).

[15] Equation (6) and (7) demonstrate that Snell's law is consistent with a stationary phase or minimum time condition, that is, Fermat's principle (see Ref. 1, p. 375.)

[16] R. A. Stephen and S. T. Bolmer, "The direct wave root in marine seismology," Bull. Seismol. Soc. Am. **75**, 57–67 (1985).

[17] R. A. Stephen and S. A. Swift, "Modeling seafloor geoacoustic interaction with a numerical scattering chamber," J. Acoust. Soc. Am. **96**, 973–990 (1994) (Fig. 5).

[18] J. N. Tjotta and S. Tjotta, "Theoretical study of the penetration of highly directional acoustic beams into sediments," J. Acoust. Soc. Am. **69**, 998–1008 (1981).

[19] F. B. Jensen and H. Schmidt, "Subcritical penetration of narrow Gaussian beams into sediments," J. Acoust. Soc. Am. **82**, 574–579 (1987).

[20] Wolfram Research, Inc., MATHEMATICA, Version 6.0, Champaign, IL, 2007.

[21] A. D. Pierce, *Acoustics: An Introduction to Its Physical Principles and Applications* (Acoustical Society of America, Melville, New York, 1989), p. 37.

[22] A. D. Pierce, *Acoustics: An Introduction to Its Physical Principles and Applications* (Acoustical Society of America, Melville, New York, 1989), p. 26.

[23] G. L. D'Spain, W. S. Hodgkiss, and G. L. Edmonds, "Energetics of the deep ocean's infrasonic sound field," J. Acoust. Soc. Am. **89**, 1134–1158 (1991).

[24] This has been questioned. See J. A. Mann III and J. Tichi, "Acoustic intensity analysis: Distinguishing energy propagation and wave-front propagation," J. Acoust. Soc. Am. **90**, 20–25 (1991); C. F. Chien and R. V. Waterhouse, "Singular points of intensity streamlines in two-dimensional sound fields," *ibid.* **101**, 705–712 (1997); however, away from singular points, it is a reasonable approximation [J. Adin Mann III, personal communication (March 14, 2005)].

[25] J. C. Osler, A. P. Lyons, P. C. Hines, J. Scrutton, E. Pouliquen, D. Jones, D. M. F. Chapman, M. O'Connor, D. Caldwell, M. MacKenzie, I. B. Haya, and D. Nesbitt, "Measuring sound speed dispersion at mid to low frequency in sandy sediments: An overview of complementary experimental techniques developed for SAX04," in Underwater Acoustic Measurements: Technologies & Results, Heraklion, Crete, Greece, Edited by J. S. Papadakis and L. Bjorno, 28 June – 1 July, 277–284 (2005).

[26] L. M. Brekhovskikh and O. A. Godin, *Acoustics of Layered Media II: Point Sources and Bounded Beams*, 2nd ed. (Springer-Verlag, Berlin, 1999) Chap. 3; O. A. Godin, N. R. Chapman, M. C. A. Laidlaw, and D. E. Hannay, "Head wave data inversion for geoacoustic parameters of the ocean bottom off Vancouver Island," J. Acoust. Soc. Am. **106**, 2540–2551 (1999).

[27] L. M. Brekhovskikh, *Waves in Layered Media, Second Edition* (Academic, Orlando, 1980), p. 281 (translated by Robert T. Beyer); L. M. Brekhovskikh and O. A. Godin, *Acoustics of Layered Media II: Point Sources and Bounded Beams*, 2nd Ed. (Springer-Verlag, Berlin, 1999), p. 19.

[28] O. A. Godin, "Transmission of low-frequency sound through the water-to-air interface," Acoust. Phys. **53**, 1063–7710 (2007).